Desalination and Water Treatment
www.deswater.com

doi: 10.5004/dwt.2017.21234

85 (2017) 197–205
August

Usage of magnetic nanoparticles coated with 3-(trimethoxysilyl)-1-propanethiol for removal of methylene blue from a textile mill wastewater

Pantea Sadat Movaseghi[a,*], Mohammad Hossein Mashhadizadeh[a], Siavash Salek Soltani[b]

[a]*Faculty of Chemistry, Kharazmi (Tarbiat Moallem) University, Tehran, Iran, Tel. +98 2122693275; email: p.movaseghi@gmail.com (P.S. Movaseghi)*
[b]*School of Chemistry, University College of Science, University of Tehran, Tehran, Iran*

Received 22 November 2016; Accepted 17 July 2017

ABSTRACT

The aim of this work was to apply iron oxide magnetic nanoparticles coated with 3-(trimethoxysilyl)-1-propanethiol, for adsorption of the cationic dye, methylene blue (MB), from aqueous solutions prior to determination with UV–Vis spectrophotometry. To approach this purpose, iron oxide magnetic nanoparticles (IOMNPs) were synthesized via co-precipitation method and characterized by Fourier transform infrared spectroscopy (FT-IR) and scanning electron microscopy. The effective parameters such as pH, time, adsorbent amount, type and volume of the desorption solvent, ionic strength of the solution and the sample volume were optimized. Figures of merit such as detection limit, relative standard deviation (RSD) and linearity range were calculated as 0.24 mg L^{-1}, 6.8% and 0.32–16 mg L^{-1}, respectively. Kinetic studies proved that adsorption process obeys pseudo-second-order model, also the adsorption isotherm was best fitted to Freundlich model with maximum adsorption capacity of 27.78 mg/g. Eventually, the method was successfully used for removing MB from a textile mill wastewater with recoveries ranging from 60% to 102%.

Keywords: Dyes; Iron oxide magnetic nanoparticles; Methylene blue; Wastewater; 3-(Trimethoxysilyl)-1-propanethiol

1. Introduction

Dyes are compounds with several uses in various industries such as textile, pulp, paper, plastic, etc., so they can be the major contaminants in industrial wastewaters. Dye production around the world is approximately 7×10^5 t annually, and textile industries discharge 1%–20% of this amount into waters [1,2]. Since dyes are colorful water pollutants, they can be recognized easily, also decrease the photosynthetic efficiency of aquatic plants due to the reduction of light penetration in water [3], increasing the biochemical oxygen demand, producing bad smell and releasing toxic effluents are other cons of these materials [4,5]. The daily increase in the world's population and limitation of water resources force humans to refine wastewaters. Hence removing dyes from wastewaters is as important as extraction of heavy metal ions.

Several wastewater treatment processes have been reported, until now. As a general point of view, these technologies include coagulation, electrocoagulation, precipitation, biodegradation, oxidation, incineration and adsorption [6–11]. Since dyes, especially, the azo ones have a high resistance to degradation, adsorption is the best way for removing them from wastewaters. Among different adsorbents for adsorption of dyes such as agricultural wastes [12–15], magnetic nanoparticles [16–19] and polymers [20–22], magnetic nanoparticles have been used a lot due to their perfect properties such as large surface to volume ratio, simple synthesis, high magnetism and being environmentally friendly. These sorbents introduced a new solid phase extraction method for preconcentration of different analytes named as magnetic solid phase extraction. This method was introduced by Safarikova et al. [23] for the first time. However solid phase extraction is a convenient preconcentration method towards other techniques such as liquid–liquid extraction because of its high sensitivity, low solvent consumption, high enrichment factor (EF), high

* Corresponding author.

recovery and simplicity. Being time consuming and tedious are some of its problems; therefore, modifying this method in a way that can save its positive criteria and also solve its problems is noticeable.

Magnetite (Fe_3O_4) adsorbents can ascend the rate of separation because of their paramagnetic properties. They are temporary magnets that have magnetism in the presence of an external magnetic field, so separation of the analyte solution from them can happen only by applying the external field.

A considerable fact about magnetic iron oxide nanoparticles is that they should be coated in order to prevent agglomeration and on the other hand become functionalized for binding to the target molecules. Different surfactants such as sodium dodecyl sulfate and cetyltrimethylammonium bromide were used by other authors [24,25].

In this study, the efforts were for the purpose of using 3-(trimethoxysilyl)-1-propanethiol (TMSPT) as a coat containing Si groups for making a linkage to oxygen atoms of Fe_3O_4 (Fig. 1) and therefore producing a long-lasting adsorbent for removing methylene blue (MB) from industrial effluents. MB is categorized as a basic dye which was first synthesized by Heinrich Caro in 1876, and its preparation was summarized by Wainwright and Giddens [26]. Although its useful applications as a dye for hair, cotton, wool and leather, redox indicator, antioxidant and antiseptic [27] attract a lot of attention, its harmful influence on human's health [28–30] makes the elimination of it from water necessary. The fascinating point is that through magnetic nanoparticles not only adsorption of MB from aqueous solutions is possible but also elution of the dye from the sorbent with ordinary organic solvents; therefore, reusability of the nanoparticles and also the dye is the other advantage of this method.

2. Experimental

2.1. Materials and reagents

All chemicals were of analytical grade and were used without any pretreatment. Methylene blue ($C_{16}H_{18}N_3S^+Cl^-$) (Fig. 2) with molecular weight of 319.85 g mol^{-1} was commercially available from Merck and its stock standard solution with the concentration of 319.85 mg L^{-1} was prepared by dissolving an appropriate amount of it in distilled water and was diluted for plotting the calibration curves. Ferric chloride hexahydrate ($FeCl_3.6H_2O$), ferrous chloride tetrahydrate ($FeCl_2.4H_2O$), ammonia solution (25%), glycerol (87%), TMSPT, methanol, glacial acetic acid, sodium chloride, ethanol and acetonitrile were purchased from Merck (Darmstadt, Germany).

2.2. Apparatus

Determination of MB was carried out by a double-beam Perkin-Elmer UV–Vis spectrophotometer (Lambda 25) at a wavelength of 665 nm. A Heidolph stirrer (Schwabach, Germany) was used for stirring the dye solution with the adsorbent. A 1.2 Tesla permanent hand-held magnet was used for separation of the IOMNPs. The pH values were adjusted with a pH/mV meter (Metrohm-827) supplied with a combined electrode. Scanning electron microscopy images were gained using a Hitachi S-4160 field emission scanning electron microscope (Tokyo, Japan). The Perkin-Elmer RXI Fourier transform infrared spectroscopy (FT-IR) spectrometer with KBr disks was applied for characterization of the bare and coated nanoparticles.

2.3. Synthesis of bare and TMSPT-coated Fe_3O_4 nanoparticles

IOMNPs were synthesized by the co-precipitation method [31]. $FeCl_3{\cdot}6H_2O$ and $FeCl_2{\cdot}4H_2O$ with 2:1 mole ratio were dissolved in 200 mL deionized water in a three-neck flask under nitrogen atmosphere and refluxed with vigorous stirring. When the temperature ascend to 85°C, 20 mL 25% ammonia solution was added to the orange-colored solution in order to change the color into black suddenly. Then the mixture was stirred for 20 min and finally IOMNPs were washed three times with 250 mL deionized water and twice with 100 mL 0.02 mol L^{-1} sodium chloride solution:

$$Fe^{2+} + 2Fe^{3+} + 8OH^- \rightarrow Fe_3O_4 \downarrow + 4H_2O$$

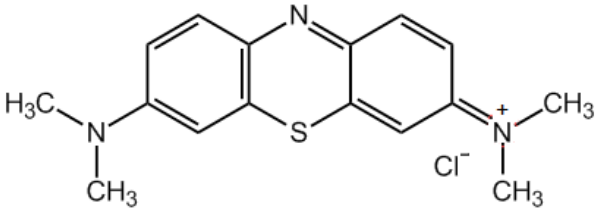

Fig. 2. Molecular structure of methylene blue.

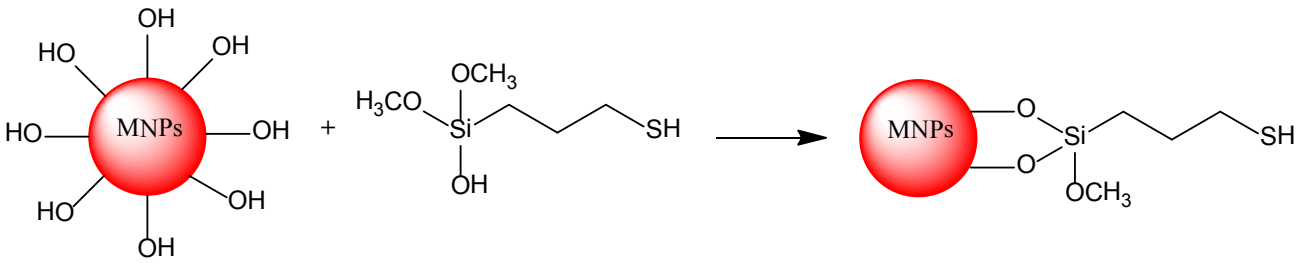

Fig. 1. Schematic diagram for the synthesis of TMSPT-coated IOMNPs.

After decantation of the supernatant, again IOMNPs were refluxed under nitrogen atmosphere and when the temperature went up to 90°C, an aqueous solution of TMSPT (10% v/v, 80 mL) was added, followed by glycerol (60 mL). The pH of the suspension was adjusted to 4.6 using glacial acetic acid, and the mixture was then stirred and heated at 90°C for 2 h. After cooling the system, TMSPT-coated IOMNPs were washed three times with 200 mL deionized water, three times with 100 mL of methanol and five times with 200 mL of deionized water. At last this adsorbent was stored in distilled water with the concentration of 40 g L^{-1}.

2.4. Dye adsorption and desorption processes

Both adsorption and desorption procedures were done by batch studies. For the adsorption step, 3 mL of the MB solution with the concentration of 3.1985 mg L^{-1} which was prepared from the standard solution was poured into a 50 mL stoppered conical flask and after adjusting the pH value at 4 by 0.1 M HCl and NaOH solutions, 0.01 g of TMSPT-coated IOMNPs was added and the solution was stirred for 20 min in order to increase the contact surface. The adsorbent was separated via the hand-held magnet at the bottom of the flask, the supernatant was decanted and the sorbent was rinsed with distilled water. For the desorption step, 2 mL of acetonitrile was added to the flask and the solution was stirred for 25 min, again the supernatant was separated using the permanent magnet and the amount of the desorbed dye was determined by UV–Vis spectrophotometer at 665 nm. The removal percentage of the dye was calculated using the following equation:

$$\%\ \text{Dye removal} = \frac{C_0 - C_t}{C_0} \times 100 \quad (1)$$

where C_0 and C_t (mg L^{-1}) are the initial dye concentration and concentration at time t, respectively.

3. Results and discussion

3.1. Characterization of the adsorbent

Transmission electron microscopy (TEM) and field emission scanning electron microscopy (FESEM) micrographs are suitable methods for specifying the size distribution and morphological structure of magnetic nanoparticles, also it can estimate the particles size too.

Fig. 3 depicts the scanning electron micrograph of TMSPT-coated IOMNPs.

As can be seen in Fig. 3, the magnetic nanoparticles have a semi-spherical morphology, with the mean diameter of 50 nm.

The FT-IR spectra of bare and TMSPT-coated IOMNPs are shown in Fig. 4. The sharp peak at 578.21 cm^{-1} in Fig. 4(a) corresponds to Fe–O band in magnetite nanoparticles which exists in Fig. 3(b) too. The broad peak at the range of 3,300–3,500 cm^{-1} belongs to the OH stretching vibrations of the hydroxyl groups and also the water molecules that adsorbed on the surface of magnetite [32]. Attachment of Si groups on to magnetic nanoparticles can be proved by the band at 1,113.32 cm^{-1} in Fig. 4(b) which corresponds to Si–O–Si stretching vibrations [33], Also the bands at 2,924 and 1,410 cm^{-1} are due to C–H stretching and CH_2 bending vibrations, respectively [34].

3.2. Optimization procedures

3.2.1. Adsorption

3.2.1.1. Influence of pH The pH parameter has a significant effect on the adsorption process. It was found that IOMNPs were oxidized when pH was below 4 [35], but coating a layer of TMSPT on the surface of the nanoparticles caused a resistance towards strong acidic conditions, so the dye removal efficiency was investigated in the range of pH 3–12. By increasing the pH, dye removal percentage was increased and reached 99% at pH 4, but after this pH no adsorption was observed until pH 12 which was

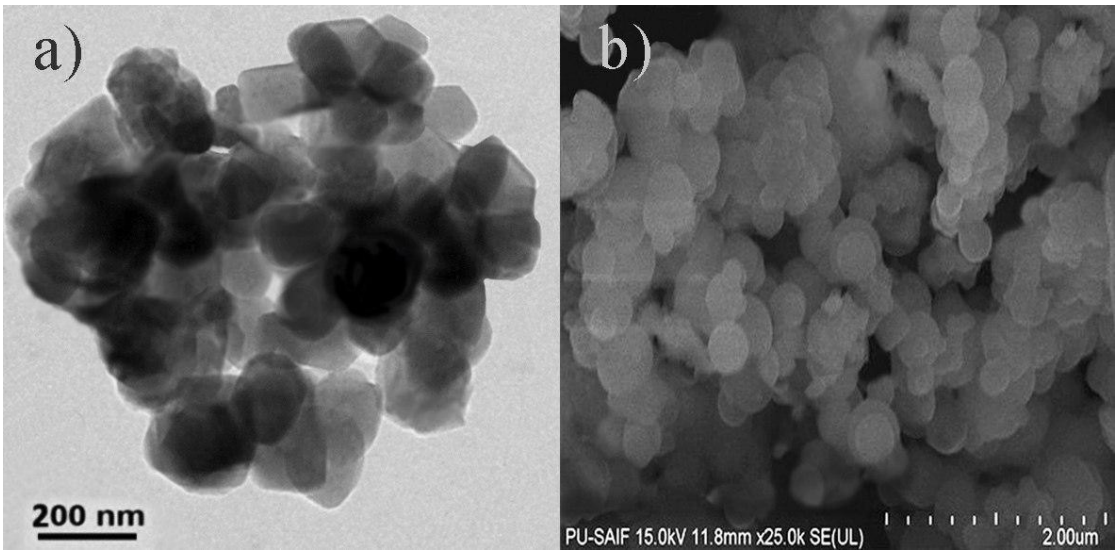

Fig. 3. (a) TEM and (b) FESEM images for TMSPT-coated IOMNPs.

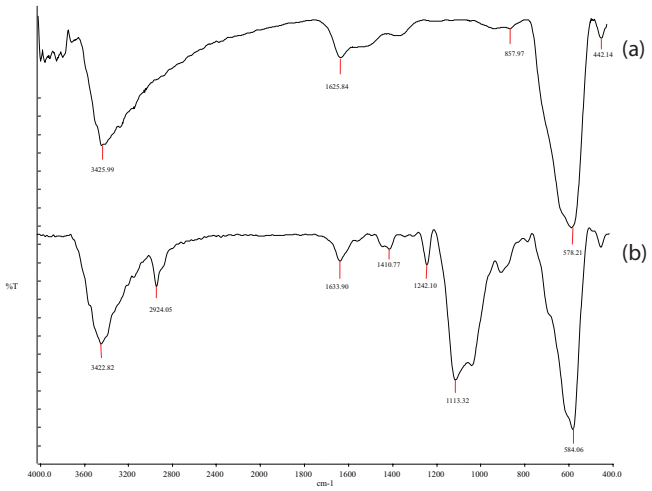

Fig. 4. FT-IR spectra of IOMNPs (a) and TMSPT-coated IOMNPs (b).

accompanied by a color change in the supernatant solution. This may be due to the separation of TMSPT coat from Fe_3O_4 NPs. Maximum adsorption capacity at pH 4 can be justified by an electrostatic interaction of the adsorbent and MB. pK_a of MB is 3.8 [36], so it has a negative charge above this value, pK_a of TMSPT is 10.55 [37] and the surface of TMSPT-coated IOMNPs has a positive charge, below this pH, therefore an electrostatic interaction between the opposite charges leads to adsorption of the adsorbate.

3.2.1.2. Effect of the adsorbent amount Amount of the adsorbent can directly affect the dye removal, because of the variation of available sites for adsorption. In order to investigate this effect, dye removal (%) was calculated by changing the MNPs amount in the range of 0.005–0.03 g. As can be seen in Fig. 5(a), removal percentage is increased when the adsorbent amount is raised to 0.01 g and after that remained constant, so 0.01 g was selected for further studies.

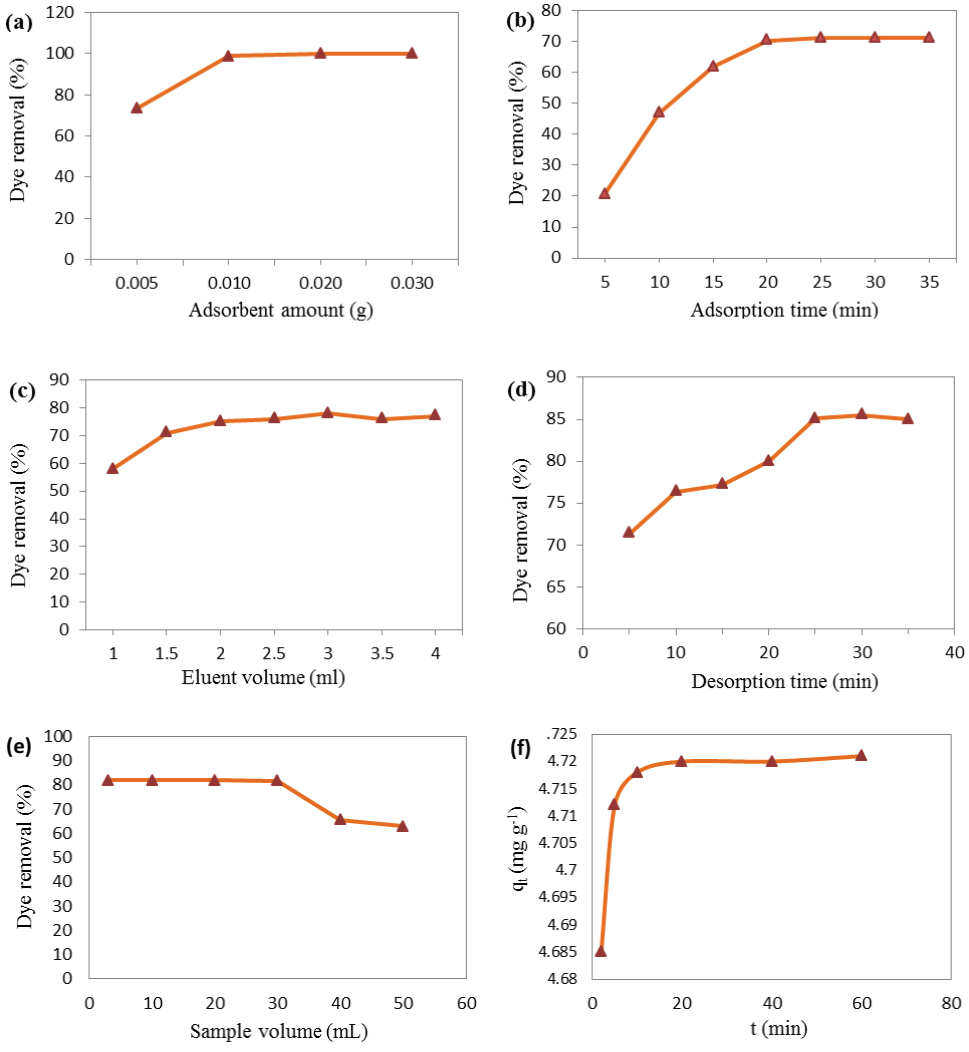

Fig. 5. Effect of (a) adsorbent amount, (b) adsorption time, (c) eluent volume, (d) desorption time, (e) sample volume and (f) time on dye removal (sample volume 3 ml, 3.1985 mg L^{-1} dye, pH 4 and 20 min adsorption).

3.2.1.3. Effect of contact time The impact of time on the adsorption process was examined by applying 5–35 min time intervals (Fig. 5(b)). As can be seen, 20 min is sufficient for complete adsorption. (Dye concentration was 10 times higher [31.985 mg L^{-1}] for better determination).

3.2.1.4. Effect of ionic strength Effect of the solution's ionic strength was followed by adding NaCl (0%–50% W/V) to the dye solution (3.1985 mg L^{-1}).The results showed that saltiness of the aqueous solution had no negative effect on the adsorption, so this adsorbent can be used even for wastewaters with high salt content. This can be justified by a change in dye's solubility, addition of a salt can decrease the solubility of the dye, hence dye molecules aggregate and precipitate on the adsorbent surface, thus adsorption capacity increases in the presence of NaCl, and in this work because of the percentage of dye adsorption (near to 100%) no result was seen by adding salt.

3.2.2. Desorption

3.2.2.1. Determination of type and volume of desorption solvent For selecting the best solvent for elution of the dye, methanol, ethanol, acetonitrile and HCl (0.1 M) were utilized. As Fig. 6 shows, maximum adsorption (up to 85%) is obtained by using acetonitrile.

Fig. 5(c) illustrates the effect of desorption solvent volume on dye removal. It is clear that 2 mL is sufficient for elution of MB from the sorbent.

3.2.2.2. Effect of time on desorption Impact of time on dye removal percentage was specified in the range of 5–35 min. Fig. 5(d) shows that 25 min is enough for 85% removal of MB.

3.2.2.3. Effect of sample volume In order to estimate the EF, the maximum amount of sample volume for a quantitative analysis should be calculated. For this purpose, sample volumes in the range of 3–50 mL were investigated. Fig. 5(e) shows that sample volumes up to 30 mL are convenient for the best dye removal.

3.2.2.4. Reusability of the adsorbent For reducing the consumption of the adsorbent from an economical point of view, they should be reusable. As it is obvious from Fig. 7, TMSPT-coated IOMNPs can be used for 10 cycles without any decrease in dye removal.

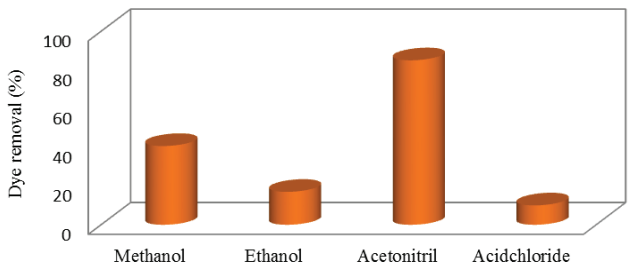

Fig. 6. Effect of eluent type on dye removal (sample volume 3 mL, 3.1985 mg L^{-1}, pH 4, 20 min adsorption, 0.01 g adsorbent and 20 min desorption).

3.3. Kinetic studies

In order to find the kinetic model which is best fitted to the experimental data, two famous kinetic models were examined: pseudo-second-order and pseudo-first-order models.

Pseudo-first-order kinetic model which was described by Lagergren [38] is presented in Eq. (2):

$$\log(q_e - q_t) = \log q_e - \frac{k_1}{2.303} t \tag{2}$$

where q_e (mg g^{-1}) and q_t (mg g^{-1}) are the amount of adsorbed dye at equilibrium and at time t (min), respectively, and k_1 (min^{-1}) is the pseudo-first-order rate constant. Plotting $\log(q_e - q_t)$ vs. t will give a straight line that its slope and intercept will give the rate constant and adsorption capacity, respectively.

The pseudo-second-order-kinetic model is introduced by Eq. (3):

$$\frac{t}{q_t} = \frac{1}{q_e} t + \frac{1}{k_2 \cdot q_e^2} \tag{3}$$

where q_e (mg g^{-1}) and q_t (mg g^{-1}) are the amount of adsorbed dye at equilibrium and at time t (min), respectively, and k_2 (min^{-1}) is the pseudo-second-order rate constant. q_e and k_2 will be derived from the slope and intercept of the plot of this formula.

Kinetic studies were carried out by adding 3 mL of MB solution with the concentration of 15.9925 mg L^{-1} to a 50 mL beaker, then 0.01 g TMSPT-coated IOMNPs were added to the solution and adsorptive uptake of the dye was followed by analyzing the supernatant after applying the permanent magnet, in time intervals ranging from 2 to 60 min. Values of q_t (mg g^{-1}) were obtained by the following equation:

$$q_t = \frac{C_0 - C_t}{m} V \tag{4}$$

where C_0 and C_t (mg L^{-1}) are the initial dye concentration and concentration at time t, respectively, m (g) is the weight of the adsorbent and V (L) is the volume of the dye solution.

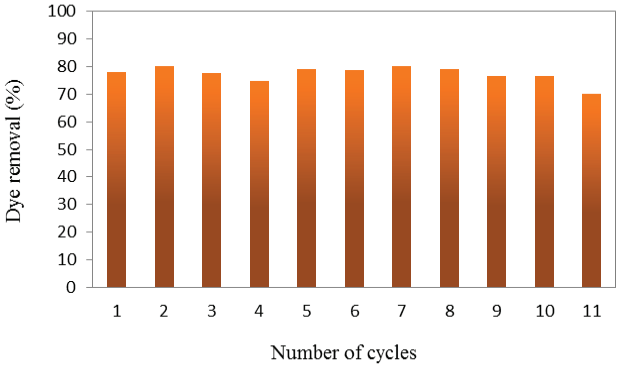

Fig. 7. Effect of number of reusability cycles on dye removal.

Fig. 5(f) shows the impact of contact time on dye adsorption. As it can be seen, at the initial minutes, rate of adsorption is rapid and after that it is changed slowly, until it reaches an equilibrium state.

The primitive rapid stage can be attributed to higher number of vacant sites, and improved concentration gradient between the dye on the adsorbent and the dye in solution [39].

Fitting the kinetic data to pseudo-first-order model and pseudo-second-order model are depicted in Fig. 8. By considering the correlation coefficients (R^2) the best model that MB adsorption obeys is the pseudo-second-order kinetic model and this means that chemisorption happens in the adsorption process.

3.4. Adsorption isotherms

In order to find the adsorption capacity of each adsorption process, it is necessary to fit the equilibrium data to the isotherm models. The two most popular adsorption isotherms are Langmuir and Freundlich. Langmuir model describes a monolayer adsorption, the sorption takes place at specific sites and the adsorbent is structurally homogeneous. The formula of Langmuir model is presented in Eq. (5).

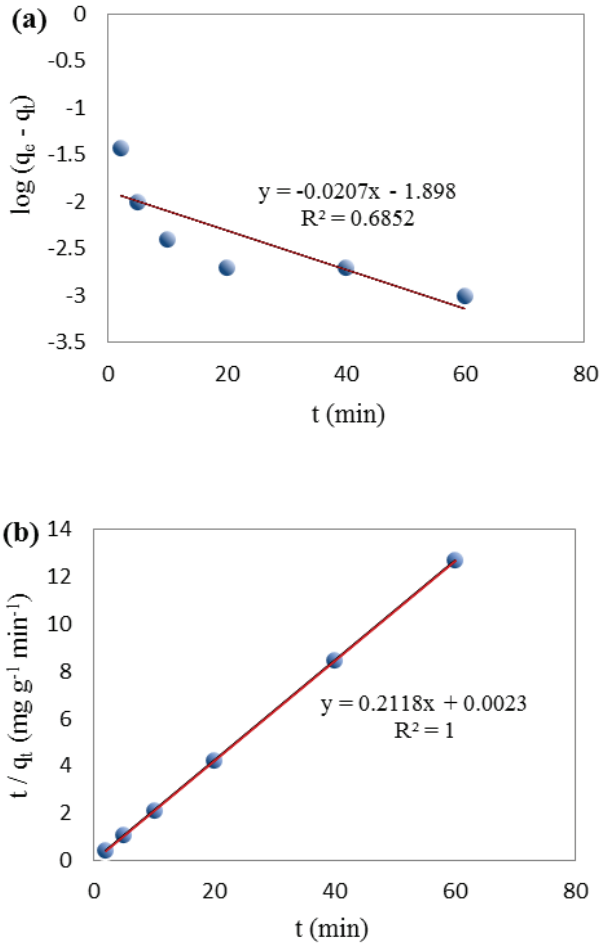

Fig. 8. Linear relationship of (a) pseudo-first-order and (b) pseudo-second-order models for adsorption of MB (3 mL dye, 15.9925 mg L^{-1} and 0.01 g adsorbent).

$$q_e = \frac{q_{\max} k_L C_e}{k_L C_e + 1} \tag{5}$$

And its linear form:

$$\frac{C_e}{q_e} = \frac{1}{q_{\max}} C_e + \frac{1}{k_L \cdot q_{\max}} \tag{6}$$

where $q_{\max}$ (mg g^{-1}) is the maximum monolayer adsorption capacity and k_L (L mg^{-1}) is the Langmuir constant. These two parameters can be obtained from the slope and intercept of the plot of C_e/q_e vs. C_e, respectively.

Freundlich isotherm has the vice versa criteria: it describes a multi-layer adsorption, a heterogeneous system exists and adsorption happens between dye and the heterogeneous surface of the sorbent [40].

Eq. (7) presents the Freundlich isotherm and its linear form is given in Eq. (8):

$$q_e = k_F \cdot C_e^{\frac{1}{n_F}} \tag{7}$$

$$\log q_e = \log k_F + \frac{1}{n_F} \log C_e \tag{8}$$

k_F (L g^{-1})and n_F are Freundlich constants, related to adsorption capacity and intensity, respectively. They can be calculated from the intercept and slope of the isotherm plot.

Studying the equilibrium of the adsorption process for finding the best isotherm model was carried out by varying the concentration of the dye solution. The same aliquots of the dye solution (3 mL) with the concentration ranging from 15.9925 to 127.94 mg L^{-1} were poured to five beakers, optimized amounts of the sorbent (0.01 g) were added to the solutions, and adsorption takes place for 20 min, then the residual dyes concentration was obtained by analyzing the supernatant at 665 nm.

Fig. 9 illustrates the plots of these two isotherm models.

As Table 1 shows, adsorption of methylene blue onto TMSPT-coated IOMNPs obeys Freundlich model (R^2 = 0.957) better than Langmuir (R^2 = 0.884) and $q_{\max}$ was 27.78 mg g^{-1}.

Results show that the surface of TMSPT-coated IOMNPs is heterogeneous and adsorption does not occur by the first layer.

3.5. Figures of merit

To determine the method validity, the analytical characteristics such as limit of detection (LOD), linearity range, RSD (%) and EF were evaluated under optimal conditions, and listed in Table 2. LOD was found 0.24 mg L^{-1} on the basis of $3S_b/m$ definition, where S_b is the standard deviation of five blank signals and m is the slope of the calibration curve for standard dye solutions. This method was found to be linear in the range of 0.32–16 mg L^{-1}. The precision of the method was investigated by calculating the RSD for five determinations and was found to be 6.8%. The EF was obtained to be 10 (30/3) by the following equation through changing the sample volume as mentioned in section 3.2.2.3:

EF = Aqueous phase volume/Eluent phase volume.

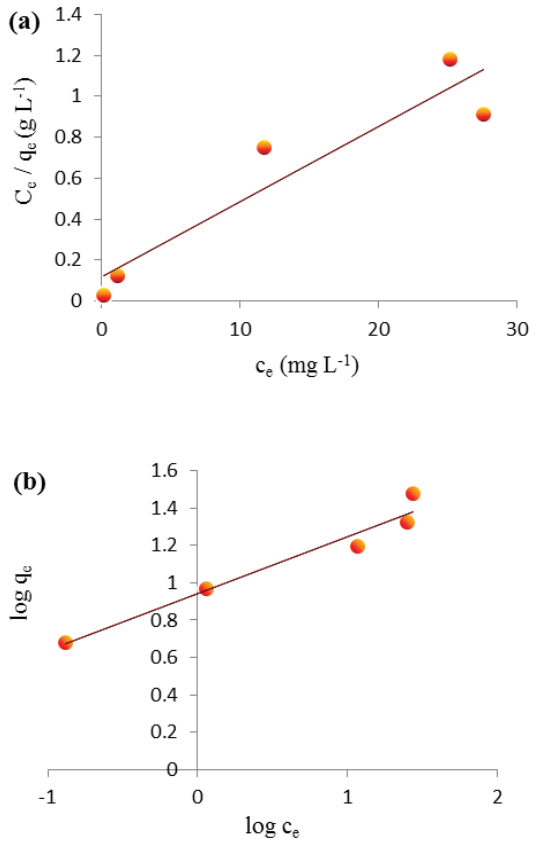

Fig. 9. (a) Langmuir and (b) Freundlich isotherm plots for adsorption of MB (3 mL dye solution, 20 min adsorption and 0.01 g adsorbent).

Table 1
Langmuir and Freundlich models parameters

Langmuir isotherm			Freundlich isotherm		
q_{max} (mg g^{-1})	k_L (L mg^{-1})	R^2	n_F	k_F (L g^{-1})	R^2
27.78	0.3053	0.884	3.268	8.690	0.957

Table 2
Analytical parameters for removal of methylene blue

LOD (mg L^{-1})	Calibration equation (R^2 = 0.998)	Linearity range (mg L^{-1})	RSD (%)
0.24	Y = 45,288 (±1,162) X + 0.003 (±0.0075)	0.32–16	6.8

3.6. Analytical applications

For specifying the validity of the proposed method for analyzing real samples, the procedure was applied to analyze a wastewater sample from a textile mill. No methylene blue was found in the real wastewater sample, so determination was carried out by spiking the dye to the solutions using the standard addition method. Table 3 shows the recoveries and RSDs for spiked samples. As can be seen, recoveries are in the range of 60%–102%, so analyzing real wastewater samples is possible by this method with satisfactory results.

Table 3
Recoveries for analyzing wastewater samples

Spiked (mg L^{-1})	Found (mg L^{-1})	Recovery % (±RSD)
0.64	0.46	73 ± 1
0.96	0.83	86 ± 4
1.28	1.30	102 ± 3
1.60	1.20	75 ± 2
1.92	1.16	60 ± 1

Table 4
Adsorption capacities for methylene blue adsorbed with different adsorbents

Adsorbent	Adsorption capacity (mg g^{-1})	References
Polymeric gel (C4)	2.61	[41]
Cashew nut shell	5.31	[42]
Mesoporous activated carbon	14.36	[43]
Spent coffee grounds	18.73	[44]
Carbonized citrus fruit peel	25.51	[45]
TMSPT-coated IOMNPs	27.78	This study

3.7. Comparison of adsorption capacity of the proposed TMSPT-coated IOMNPs with other adsorbents

The adsorption capacity of the magnetite nanoparticles coated with 3-(trimethoxysilyl)-1-propanethiol is compared with other sorbents and listed in Table 4.

4. Conclusion

In this work, iron oxide magnetic nanoparticles were coated with a new thiol compound. This adsorbent could successfully adsorb the cationic dye, methylene blue, from real wastewater samples with high recoveries and without the effect of samples' salt contents. The adsorption capacity of 27.78 (mg g^{-1}) was obtained for the sorbent which is comparable with the referenced works. Desorption of the dye can be achieved simply, and reusability of the adsorbent made this method cost-effective. Kinetic and isothermal studies proved that adsorption process obeys pseudo-second-order model and Freundlich isotherm. Finally the method was validated by calculation of detection limit, repeatability and linearity range.

Acknowledgments

The authors appreciate support of this work by Kharazmi University and also University of Tehran.

References

[1] M. Anbia, S. Salehi, Removal of acid dyes from aqueous media by adsorption onto amino-functionalized nanoporous silica SBA-3, Dyes Pigm., 94 (2012) 1–9.

[2] S. Xiong, M. Qiu, J. Son, G. Wang, Y. Xuan, Z. Wang, Adsorption isotherm and equilibrium process of dye wastewater onto camphor sawdust, Nat. Environ. Pollut. Technol., 15 (2016) 689–692.

[3] W. Zhang, L. Ding, J. Luo, M.Y. Jaffrin, B. Tang, Membrane fouling in photocatalytic membrane reactors (PMRs) for water and wastewater treatment: a critical review, Chem. Eng. J., 302 (2016) 446–458.

[4] S. Sharma, P. Malaviya, Bioremediation of tannery wastewater by chromium resistant novel fungal consortium, Ecol. Eng., 91 (2016) 419–425.

[5] D. Pokhrel, T. Viraraghavan, Treatment of pulp and paper mill wastewater—a review, Sci. Total Environ., 333 (2004) 37–58.

[6] A. Jamali, A.A. Tehrani, F. Shemirani, A. Morsali, Lanthanide metal–organic frameworks as selective microporous materials for adsorption of heavy metal ions, Dalton Trans., 45 (2016) 9193–9200.

[7] M. Chethana, L.G. Sorokhaibam, V.M. Bhandari, S. Raja, V.V. Ranade, Green approach to dye wastewater treatment using biocoagulants, ACS Sustain. Chem. Eng., 4 (2016) 2495–2507.

[8] C.Y. Teh, P.M. Budiman, K.P.Y. Shak, T.Y. Wu, Recent advancement of coagulation–flocculation and its application in wastewater treatment, Ind. Eng. Chem. Res., 55 (2016) 4363–4389.

[9] X. Dong, Y. Wang, X. Li, Y. Yu, M. Zhang, Process simulation of laboratory wastewater treatment via supercritical water oxidation, Ind. Eng. Chem. Res., 53 (2014) 7723–7729.

[10] S.K. Gupta, M.K. Nayunigari, R. Misra, F.A. Ansari, D.D. Dionysiou, A. Maity, F. Bux, Synthesis and performance evaluation of a new polymeric composite for the treatment of textile wastewater, Ind. Eng. Chem. Res., 55 (2016) 13–20.

[11] T. Jiao, H. Zhao, J. Zhou, Q. Zhang, X. Luo, J. Hu, Q. Peng, X. Yan, Self-assembly reduced graphene oxide nanosheet hydrogel fabrication by anchorage of chitosan/silver and its potential efficient application toward dye degradation for wastewater treatments, ACS Sustain. Chem. Eng., 3 (2015) 3130–3139.

[12] S.F. Kamazani, S.S. Soltani, A. Zonouzi, Highly efficient synthesis of new 2H-chromene dyes using Cu-SBA-15, Orient. J. Chem., 32 (2016) 2543–2548.

[13] C.C. Escobar, A. Fisch, J.H.Z. Santos, Effect of a sol–gel route on the preparation of silica-based sorbent materials synthesized by molecular imprinting for the adsorption of dyes, Ind. Eng. Chem. Res., 54 (2015) 254–262.

[14] L. Liu, Z.Y. Gao, X.P. Su, X. Chen, L. Jiang, J.M. Yao, Adsorption removal of dyes from single and binary solutions using a cellulose-based bioadsorbent, ACS Sustain. Chem. Eng., 3 (2015) 432–442.

[15] L. Ai, L. Li, Efficient removal of organic dyes from aqueous solution with ecofriendly biomass-derived carbon@ montmorillonite nanocomposites by one-step hydrothermal process, Chem. Eng. J., 223 (2013) 688–695.

[16] X. Li, Z. Niu, J. Jiang, L. Ai, Cobalt nanoparticles embedded in porous N-rich carbon as an efficient bifunctional electrocatalyst for water splitting, J. Mater. Chem. A, 4 (2016) 3204–3209.

[17] A.L. Cazetta, O. Pezoti, K.C. Bedin, T.L. Silva, A.P. Junior, T. Asefa, V.C. Almeida, Magnetic activated carbon derived from biomass waste by concurrent synthesis: efficient adsorbent for toxic dyes, ACS Sustain. Chem. Eng., 4 (2016) 1058–1068.

[18] A. Dolatkhah, L.D. Wilson, Magnetite/polymer brush nanocomposites with switchable uptake behavior toward methylene blue, ACS Appl. Mater. Interfaces, 8 (2016) 5595–5607.

[19] Z. Cheng, J. Liao, B. He, F. Zhang, F. Zhang, X. Huang, L. Zhou, One-step fabrication of graphene oxide enhanced magnetic composite gel for highly efficient dye adsorption and catalysis, ACS Sustain. Chem. Eng., 3 (2015) 1677–1685.

[20] L. Ai, X. Gao, J. Jiang, *In situ* synthesis of cobalt stabilized on macroscopic biopolymer hydrogel as economical and recyclable catalyst for hydrogen generation from sodium borohydride hydrolysis, J. Power Sources, 257 (2014) 213–220.

[21] E.F. Molina, R.L.T. Parreira, E.H. Faria, H.W.P. Carvalho, G.F. Caramori, D.F. Coimbra, E.J. Nassar, K.J. Ciuffi, Ureasil-poly(ethylene oxide) hybrid matrix for selective adsorption and separation of dyes from water, Langmuir, 30 (2014) 3857–3868.

[22] S. Majumdar, U. Saikia, D. Mahanta, Polyaniline-coated filter papers: cost effective hybrid materials for adsorption of dyes, J. Chem. Eng. Data, 60 (2015) 3382–3391.

[23] M. Safarikova, I. Safarik, Magnetic solid-phase extraction, J. Magn. Magn. Mater., 194 (1999) 108–112.

[24] E. Ranjbari, M.R. Hadjmohammadi, F. Kiekens, K. Wael, Mixed hemi/ad-micelle sodium dodecyl sulfate-coated magnetic iron oxide nanoparticles for the efficient removal and trace determination of rhodamine-B and rhodamine-6G, *Anal. Chem.*, 87 (2015) 7894–7901.

[25] T. Jurkin, M. Gotic, G. Stefanic, I. Pucic, Gamma-irradiation synthesis of iron oxide nanoparticles in the presence of PEO, PVP or CTAB, Radiat. Phys. Chem., 124 (2016) 75–83.

[26] M. Wainwright, R.M. Giddens, Phenothiazinium photosensitisers: choices in synthesis and application, Dyes Pigm., 57 (2003) 245–257.

[27] A. Aluigi, G. Sotgiu, A. Torreggiani, A. Guerrini, V.T. Orlandi, F. Corticelli, G. Varchi, Methylene blue doped films of wool keratin with antimicrobial photodynamic activity, ACS Appl. Mater. Interfaces, 7 (2015) 17416–17424.

[28] M. Oz, D. Isaev, D. Lorke, M. Hasan, G. Petroianu, T. Shippenberg, Methylene blue inhibits function of the 5-HT transporter, Br. J. Pharmacol. Chemother., 166 (2012) 168–176.

[29] L. Hencken, J.A. Morgan, Serotonin syndrome following methylene blue administration for vasoplegic syndrome, J. Card. Surg., 31 (2016) 208–210.

[30] Z. Jia, Z. Li, S. Li, Y. Li, R. Zhu, Adsorption performance and mechanism of methylene blue on chemically activated carbon spheres derived from hydrothermally-prepared poly(vinyl alcohol) microspheres, J. Mol. Liq., 220 (2016) 56–62.

[31] M.H. Mashhadizadeh, M.A. Diva, M.R. Shapouri, H. Afruzi, Solid phase extraction of trace amounts of silver, cadmium, copper, mercury, and lead in various food samples based on ethylene glycol bis-mercaptoacetate modified 3-(trimethoxysilyl)-1-propanethiol coated Fe_3O_4 nanoparticles, Food Chem., 151 (2014) 300–305.

[32] D. Creanga, G. Calugaru, Physical investigations of a ferrofluid based on hydrocarbons, J. Magn. Magn. Mater., 289 (2005) 81–83.

[33] G. Liu, M. Cai, X. Wang, F. Zhou, W. Liu, Core–shell–corona-structured polyelectrolyte brushes-grafting magnetic nanoparticles for water harvesting, ACS Appl. Mater. Interfaces, 6 (2014) 11625–11632.

[34] S. Rashidi, A. Ataie, Structural and magnetic characteristics of PVA/$CoFe_2O_4$ nano-composites prepared via mechanical alloying method, Mater. Res. Bull., 80 (2016) 321–328.

[35] X.L. Zhao, Y.L. Shi, Y.Q. Cai, S.F. Mou, Cetyltrimethylammonium bromide-coated magnetic nanoparticles for the preconcentration of phenolic compounds from environmental water samples, Environ. Sci. Technol., 42 (2008) 1201–1206.

[36] X. He, K. Male, P. Nesterenko, D. Brabazon, B. Paull, J. Luong, Adsorption and desorption of methylene blue on porous carbon monoliths and nanocrystalline cellulose, ACS Appl. Mater. Interfaces, 5 (2013) 8796–8804.

[37] G.C. Shields, P.G. Seybold, Computational Approaches for the Prediction of pK_a Values, CRC Press, New York, 2014.

[38] S. Lagergren, Zur theorie der sogenennten adsorption geloster stoffe, K. Sven. Vetensk.adad. Handl., 24 (1898) 1–39.

[39] E. Forgacs, T. Cserhati, G. Oros, Removal of synthetic dyes from wastewaters: a review, Environ. Int., 30 (2004) 953–971.

[40] G. Crini, P.M. Badot, Application of chitosan, a natural aminopolysaccharide, for dye removal from aqueous solutions by adsorption processes using batch studies: a review of recent literature, J. Prog. Polym. Sci., 33 (2008) 399–447.

[41] M.A. Malana, S. Ijaz, M.N. Ashiq, Removal of various dyes from aqueous media onto polymeric gels by adsorption process: their kinetics and thermodynamics, Desalination, 263 (2010) 249–257.

[42] P.S. Kumar, R.V. Abhinaya, K.G. Lashmi, V. Arthi, R. Pavithra, V. Sathyaselvabala, S.D. Kirupha, S. Sivanesan, Adsorption of methylene blue dye from aqueous solution by agri-cultural waste: equilibrium, thermodynamics, kinetics, mechanism and process design, Colloid J., 73 (2011) 651–661.
[43] J.S. Macedo, N.B. Costa Junior, L.E. Almeida, E.F.S. Vieira, A.R. Cestari, I.F. Gimezez, N.L.V. Carre˜no, L.S. Barreto, Kinetic and calorimetric study of the adsorption of dyes on mesoporous activated carbon prepared from coconut coir dust, J. Colloid Interface Sci., 298 (2006) 515–522.
[44] A.S. Franca, L.S. Oliveira, M.E. Ferreira, Kinetics and equilibrium studies of methylene blue adsorption by spent coffee grounds, Desalination, 249 (2009) 267–272.
[45] S. Dutta, A. Bhattacharyya, A. Ganguly, S. Gupta, S. Basu, Application of response surface methodology for preparation of low-cost adsorbent from citrus fruit peel and for removal of methylene blue, Desalination, 275 (2011) 26–36.